Orbital
The electronic journal of chemistry

the electronic journal of chemistry

Full paper | http://dx.doi.org/10.17807/orbital.v14i2.16192

The Efficacy of New Liquid Laser Dye Material – Chalcone: 1-(4-methylsulfonyl phenyl)-3-(4-*N,N*-dimethyl (amino phenyl)-2-propen-1-one (MSPPP)

Mohana Attia* [a] and Abdelrahman A. Elbadawi [b]

This paper includes the efficacy of synthesis and characterization of a new liquid laser dye material – chalcone of 1-(4-methylsulfonyl phenyl)-3-(4-*N,N*-dimethyl (amino phenyl)-2-propen-1-one (MSPPP) and its application as a new laser medium. The absorption and fluorescence spectra of MSPPP were investigated under different solvents and concentrations. The study investigated the pump pulse energies of Nd: YAG laser (355 nm) and the amplified spontaneous emission (ASE) performance of MSPPP under various concentrations, and organic solvents. At identical conditions, the amplified spontaneous emission spectra of MSPPP in solution were compared with a conventional laser dye of coumarin 503. The fluorescence quantum yield and the gain of MSPPP were determined. The features are: (I) MSPPP has stellar photochemical stabilization., (II) ASE from the MSPPP was setting in the wavelength range between 515 and 548 nm. The molecular geometry was optimized and their HOMO– LUMO energy values were determined by SCM Software for Chemistry & Materials using DFTB (GGA BLYP) [Density-Functional based Tight-Binding] method.

Graphical abstract

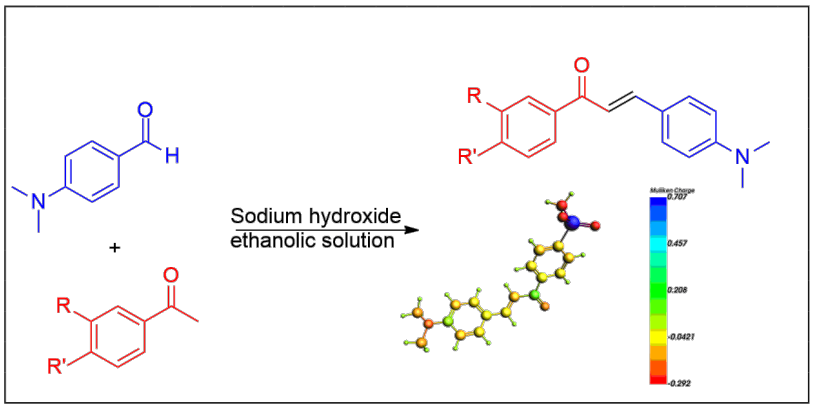

Keywords

Amplified Spontaneous Emission
DFTB
Energy gap
MSPPP Chalcone
Quantum yield of fluorescence
Stokes shift

Article history

Received 18 Aug 2021
Revised 28 Jan 2022
Accepted 18 Apr 2022
Available online 03 Jul 2022

Handling Editor: Adilson Beatriz

1. Introduction

Chalcones exemplify a substantial family of natural as well as synthetic organic compounds, first, isolated from the Chinese liquorice [1]. Chalcones and their derivatives are a significant set of natural products and have been reported to possess various biological and pharmacological effects [2]. These chalcones have encouraged broad research owing to their unique structure, which includes a carbonyl functional group conjugated to a carbon-carbon double bond. This structural arrangement gives rise to numerous chemical, physical, photophysical and biological properties [2-8]. In 2002, Yah et al [9] prepared a series of chalcone derivatives, which displays 90 % inhibitory activity against *Mycobacterium*

[a] Shaqra University, PYP, QEC, Department of Physics, Saudi Arabia. [b] Department of physics, Physics College/School of Physics/ Alneelain University, Khartoum, Sudan. *Corresponding author. E-mail: **matiah@su.edu.sa**

tuberculosis. The first report on chalcones and related compounds as an optical material is traced back to a few decades by Kitaoka et al [10]. Later, Fabian et al [11] (2003), synthesized 10 compounds and studied for leishmanicidal and trypanocidal activity, among those, 5 compounds displayed prominent and inhibitory effect on the growth of *Trypanosome cruzi* and only 2 compounds showed potent inhibitory activity on the growth of *L. braziliensis* in vitro. Recent records related to chalcones are most applied on optical applications (OA) through second harmonic generation materials in nonlinear optics (NLO) and fluorescent probes for sensing of metal ions [12-21]. However, the photophysical properties of these chalcones like temperature effect, the quantum yield of fluorescence, and solvent environment, were not completely investigated. Therefor in the present paper, we prepared the chalcone 1-(4-methylsulfonyl phenyl)-3-(4-N, N dimethyl (amino phenyl)-2-propen-1-one (MSPPP) (Scheme 1) and analyzed its photophysical properties and amplified spontaneous emission (ASE) as well as its photochemical stability, in different solvents and concentrations.

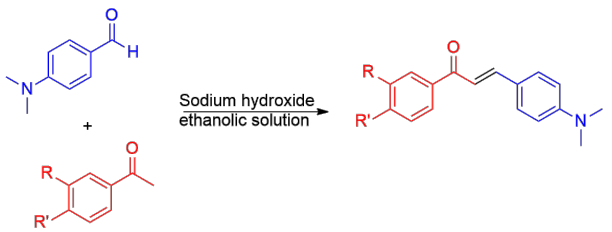

MSPPP, R = H, R1 = Me

Scheme 1. Chemical reaction of chalcones preparation.

2. Material and Methods

2.1 Chemical synthesis and characterization

A green synthesis of chalcones was performed using a condensation reaction of 4- dimethylamino benzaldahyde (0.01 mol) 1-(4-(methylsulfonyl)phenyl)ethan-1-one (0.01 mol) in a basic solution of sodium hydroxide (1.0 gm) and ethanol (50 ml). From ethanol and water, the compound was recrystallized, and filtered, washed with water, and left to dry.

MSPPP Chalcone confirmed by H^1 NMR and UV – Vis spectroscopy, (400 MHz) ^{1}H NMR: δ 2.86 (6H, s), 3.07 (3H, s), 6.47 (1H, d, J = 15.6 Hz), 6.84 (2H, ddd, J = 8.2, 1.2, 0.4 Hz), 7.47-7.58 (3H, 7.51 (d, J = 15.6 Hz), 7.55 (ddd, J = 8.2, 1.5, 0.5 Hz)), 7.81 (2H, ddd, J = 7.9, 1.9, 0.5 Hz), 8.01 (2H, ddd, J = 7.9, 1.5, 0.5 Hz). λmax (methanol 419 nm).

2.2 Spectral analysis

In different organic solvents, MSPPP was dissolved (a spectroscopic grade with purity 99.8%). Figure 1 is shown the molecular structure of MSPPP. Under a wide range of concentrations, the absorption and fluorescence spectra of MSPPP in acetone were studied. Using a small quartz cuvette with the dimensions 1 × 1 × 4 cm^3 with an optical path length of 1 cm the spectra of these solutions were measured. For measuring the absorption spectra were using a Perkin-Elmer LAMBDA 590 spectrophotometer with a wavelength range from 200 to 800 nm. The fluorescence spectra were measured by a Perkin-Elmer LS55 spectrofluorometer, with a wavelength range of 200 to 900 nm, at room temperature. The excitation wavelength was 400 nm. The UV laser (λ = 355 nm) was focused by a quartz plan cylindrical lens with a focal length of 5 cm. The amplified spontaneous emission (ASE) of the MSPPP in solution was compared to that of coumarin 503 (see Fig. 1) in ethanol.

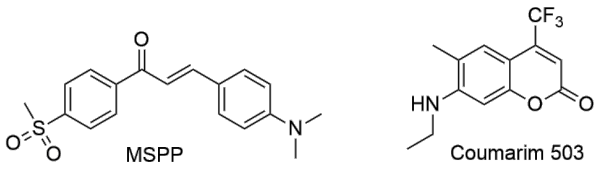

Fig. 1. Molecular structure: MSPPP and coumarin 503.

3. Results and Discussion

3.1 Spectral characteristic of MSPPP

MSPPP was dissolved diverse organic solvents with various dielectric constants (Table 1). The solutions' concentration was fixed at 6.5 mM. Both absorption and emission spectra of MSPPP show a large redshift as the solvent polarity is raised. In the absorption and fluorescence bands, it could be seen that the dielectric constant of the solvent plays an important role. Table 1 displays the influence of solvents on the absorption and fluorescence spectra.

Table 1. Data of the impact of the solvents on the absorption and fluorescence spectra.

Solvent	ε	λ_{max}			ϕ_F	η
		A	F	ASE		
Methanol	32.5	420	530	-----	0.02	----
Ethanol	24.2	419	529	548	0.35	3.8
Acetone	20.5	406	517	522.5	0.85	30
Toluene	2.6	405	472	-----	0.22	----
Benzene	2.23	406	475	-----	0.26	----
Tetrahydrofuran (THF)	7.55	402	504	511	0.98	45
Dimethylformamide (DMF)	36.7	415	527.5	541	0.96	34

ε is the dielectric constant, spectral and ASE properties: λ_{max} (nm) for absorption (A), F is the fluorescence and ASE; ϕ_F; ASE efficiency η (%) of MSPPP.

An early study reported that the intensity of the fluorescence decreases significantly as the concentration of the similarly compounds MSPPP increased [22]. With an increase in concentration, the optical density of the absorption

increased, although regardless of the concentration, the shape of the absorption spectra remained the same.

3.1.1 Stokes shift

The variations in the absorption and fluorescence spectra were observed. The variation of the Stokes shift as a function of the dipole factor of the solvent, as defined by Lippert and Mataga et al. [23] is shown in Fig 2. It can be noticed that MSPPP in solution undergoes considerable changes in the electron delocalization and becomes strongly polar in the excited state when compared the ground state. The Stokes shift has a linear variation with the dipole factor, which is written in the expression:

$$v_a - v_f \approx \left(\frac{(\varepsilon-1)}{(2\varepsilon+1)} - \frac{(n^2-1)}{(2n^2+1)}\right)\frac{(\mu_e-\mu_g)^2}{a^3hc} \quad (1)$$

$$D_f = \frac{(\varepsilon-1)}{(2\varepsilon+1)} - \frac{(n^2-1)}{(2n^2+1)} \quad (2)$$

where D_f is dipole factor, v_a and v_f are the absorption and fluorescence peaks in wave numbers respectively, ε is the dielectric constant and n is the solvents refractive index. μ_e is the dipole moment of the solute in the excited state. μ_g is representing the dipole moment of the solute the ground states, respectively, and a is the radius of the solvent cage around the solute.

The Stokes shift as a function of dipole factor in representative solvents is shown in Fig. 2. This dipole factor is a gauge of dipole − dipole interaction between the solvents and the solute. Under the same identical condition, one can readily see that MSPPP is more polar than coumarin 503. The MSPPP change is much greater than coumarin 503, implying that MSPPP shows a great change in the dipole moment in the excited state.

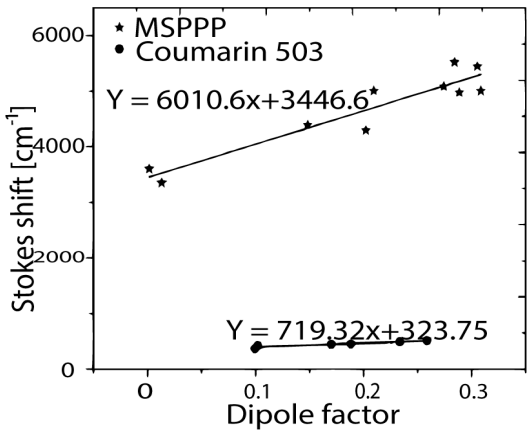

Fig. 2. Variation in the Stokes shift of MSPPP and coumarin 503.

3.1.2 Fluorescence quantum yield

By diluted solutions, the fluorescence quantum yields (ΦF) of MSPPP and coumarin 503 were measured. For each solution, the concentration was preserved at 0.65 mM. By the following expression, the quantum yield can be calculated [24].

$$\phi_f(S) = \phi_f(R)\frac{A_R n_S^2 \int I_S(\bar{v})dv}{A_S n_R^2 \int I_R(\bar{v})dv} \quad (3)$$

where the indices ***S*** and ***R*** refer to the sample and reference, respectively, and the integral over I represent the area under the fluorescence spectrum. A is the optical density, and n is the refractive index of the solvents.

Table 1 and 2 show the quantum yields of fluorescence (ΦF) for MSPPP and coumarin 503. The ΦF of MSPPP is higher than that of coumarin 503 under identical conditions.

3.1.3 Amplified spontaneous emission

MSPPP was dissolved in acetone at a concentration of 2 mM, to study the ASE characteristics of MSPPP under high power excitation. With a UV laser, this solution was transversely excited. Figure 3 shows the ASE spectrum was listed at 532 nm with a tight spectral bandwidth of 6 nm (FWHM) at a pump power of 9 mJ. At this concentration, this ASE peak is coinciding with the maximum of the fluorescence emission spectrum. There was no significant redshift observed when the concentration increased to 6 mM.

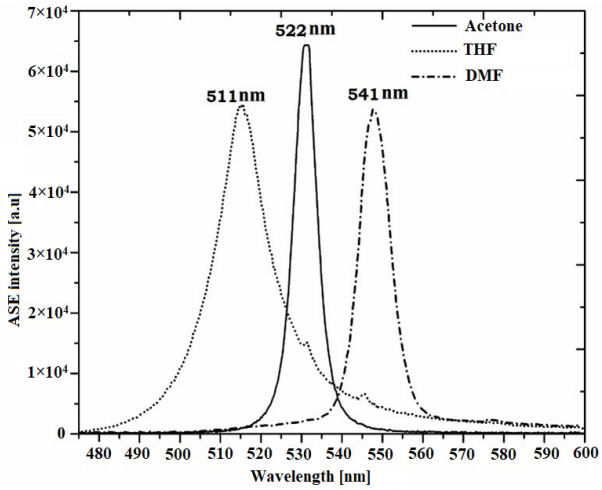

Fig. 3. ASE spectra of MSPPP in acetone, tetrahydrofuran (THF), and Dimethylformamide (DMF).

By a gen-tec energy meter, the ASE efficiency of MSPPP in acetone was calculated. 9 mJ is the input energy. By focusing laser energy as a stripe of light on the cuvette, the sample was excited transversal. On both sides of the cuvette, ASE was emitting as a cone of intense light vertically to laser excitation. 2.8 mJ is the energy of ASE after being measured. in diverse solvents, in a similar fashion, the ASE efficiency of MSPPP was calculated. Table 2 shows that the ASE efficiency depends on the solvent environments. At concentration 2mM and the pump power energy 9 mJ, Table 2 shows the ASE spectra of MSPPP in different solvents having different polarities under identical conditions. Figure 3 indicate that when the dielectric constant raised, the emission wavelength increasingly red shifted. Additionally, at high pump power energy and concentration the ASE in methanol, benzene, acetic acid, and toluene was not revealed. In benzene and toluene this may do be due to the lower solubility of the MSPPP for these solvents. In acetic acid, the absence of the ASE spectra may do be due to the protonation of N-dimethylamino group of MSPPP with responsible for their photo characteristic. Through hydrogen bonding the methanol plays identical role by suppression of the lone pair of N-dimethylamino group, this slightly appears in ethanol which gives poor ASE. Table 2 shows the results were compared with coumarin 503 as standard material.

Table 2. Coumarin 503 in different solvent.

Solvent	ε	λ_{max}			ϕ_F	η
		A	F	ASE		
Methanol	32.7	394	490	500	0.42	9.6
Ethanol	24.5	393	492	502	0.37	16
Acetone	20.5	389	489	496	0.53	14
Toluene	2.6	378	455	465	0.21	7
Benzene	2.23	377	449	459	0.26	9
tetrahydrofuran	7.55	384	476	485	0.40	11

ε is the dielectric constant, spectral and ASE properties: λ_{max} (nm) for absorption (A), F is the fluorescence and ASE; ϕF; ASE efficiency η (%) of coumarin 503 in different solvent.

From 2 to 6 mM the concentration was taken, the variation in the ASE intensities of MSPPP as a function of the concentration is shown in Fig. 4. The solvents were dimethylformamide (DMF), tetrahydrofuran (THF), and acetone. The intensity of the ASE decreased for each solution with the concentration raised when the pump power was 9 mJ.

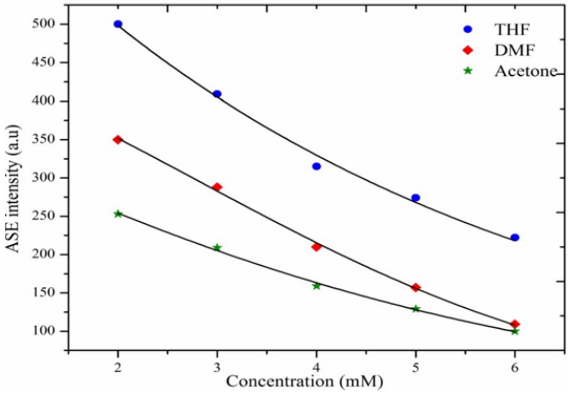

Fig. 4. ASE intensities of MSPPP in DMF, acetone, and THF.

Under identical conditions, the comparison of the ASE intensity of MSPPP dissolved in acetone, DMF and THF is shown in Fig. 5. These solvents have been chosen because they give high ASE intensities. Moreover, they represent high medium, and low dielectric constants. The concentration was kept at 2 mM for each solution, and the pump power was taken from 3 to15 mJ. It was found that as the pump power was increased, the intensity of MSPPP in acetone increased slowly, while in THF the intensity increased rapidly.

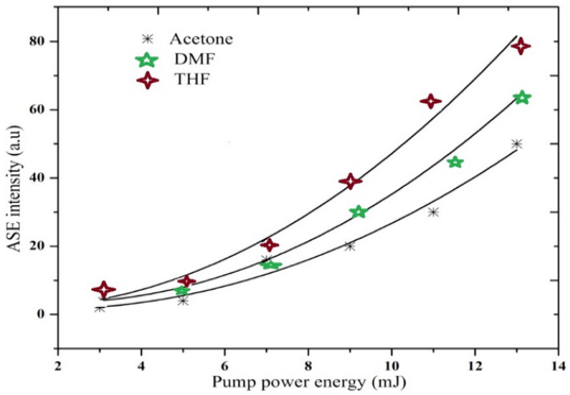

Fig. 5. ASE intensities of MSPPP in DMF, acetone, and tetrahydrofuran (THF).

At a concentration of 2 mM, the photochemical stabilization of the MSPPP in DMF was compared to that of coumarin 503 in ethanol. With pulse energy of 9 mJ and a repetition rate of 10 Hz, these solutions were pumped by UV laser of Nd: YAG. Figure 6 shows the ASE intensity of MSPPP remained constant after 3000 pulses, whereas that of coumarin 503 dropped to 50% of the initial intensity after 3000 pulses and disappeared completely at 7000 pulses.

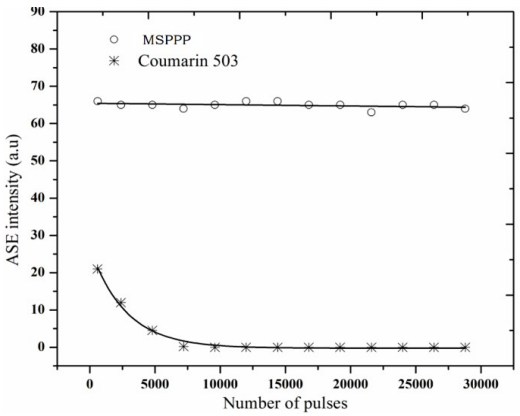

Fig. 6. The photochemical stability of MSPPP in DMF and coumarin 503 in ethanol.

Under the same operating conditions, the photochemical stability of MSPPP in different solvents was studied. Figure 7 shows the ASE intensity of THF, and acetone was dropped to 32% and 25%, respectively after 3000 pulses. At the concentration of 2 mM, the optical gain of MSPPP in DMF was measured. In ethanol, the Coumarin 503 was prepared. From 3 mJ to 15 mJ the pump pulse energy was varied; the excitation wavelength was 355 nm. For two lengths of excitation L1 = 0.5 cm and L2 = 0.3 cm, the ASE intensity was measured [25].

$$\frac{I_1}{I_2} = \frac{e^{\gamma L_1} - 1}{e^{\gamma L_2} - 1} \quad (4)$$

where L is the length of excitation and γ is the optical gain.

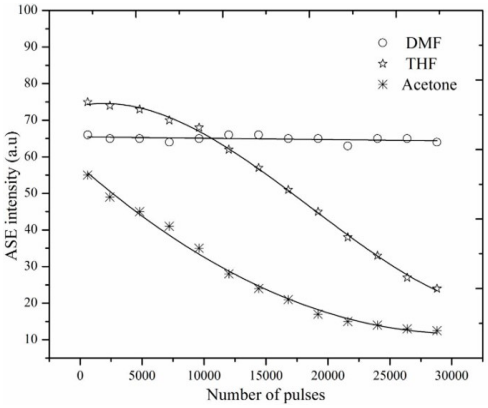

Fig. 7. The photochemical stability of MSPPP in three different solvents at a concentration of 2 mM.

Figure 8 shows the optical gain of MSPPP in DMF is higher

than the coumarin 503 in ethanol.

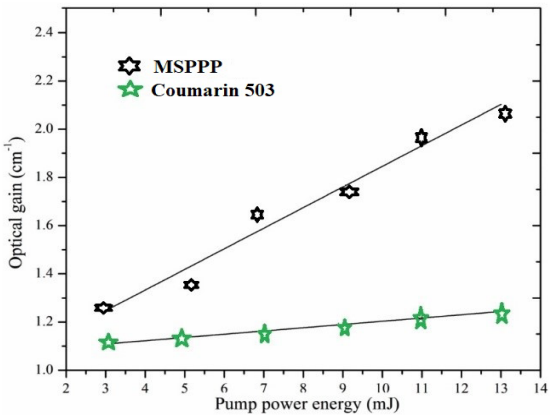

Fig. 8. The relationship between the optical gains vs. pump pulse energy for MSPPP in DMF and coumarin 503 in ethanol at a concentration of 0.6 mM.

3.2 Quantum chemical calculation

The molecular geometry was optimized and their HOMO–LUMO energy values were determined by SCM Software for Chemistry & Materials using DFTB (GGA BLYP) [Density-Functional based Tight-Binding] method. The theoretical data, including the highest occupied molecule orbital (HOMO) and the lowest unoccupied molecule orbital (LUMO) transition, molecule dipole moment (μ_D), and the energy band gaps (Eg) values for MSPPP molecule is tabulated in "Table 3". Figures 9, 10 and 11 show the HOMO – LUMO, HOMO – LUMO excitation and the electron distribution for MSPPP was performed using the Mullikan method, respectively.

Table 3. Structural parameters of the organic ligand: Dipole Moment (μD), Energy, EHOMO, ELUMO, Egap.

μ_D	Energy (eV)	E_{HOMO} (eV)	E_{LUMO} (eV)	E_{gap} (eV)
6.13	-281	-1.90	-0.177	1.73

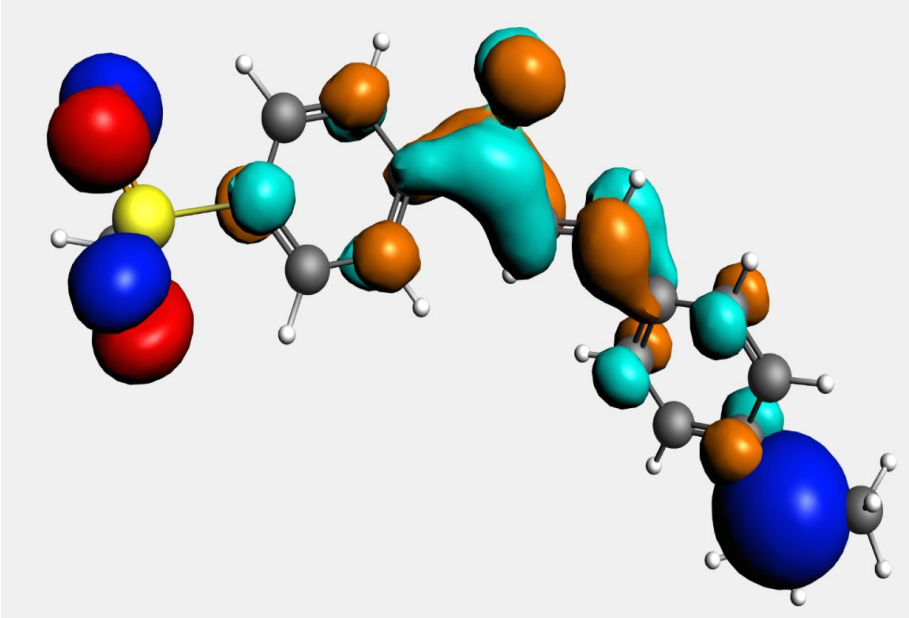

Fig. 9. The molecule orbital HOMO – LUMO diagram of MSPPP.

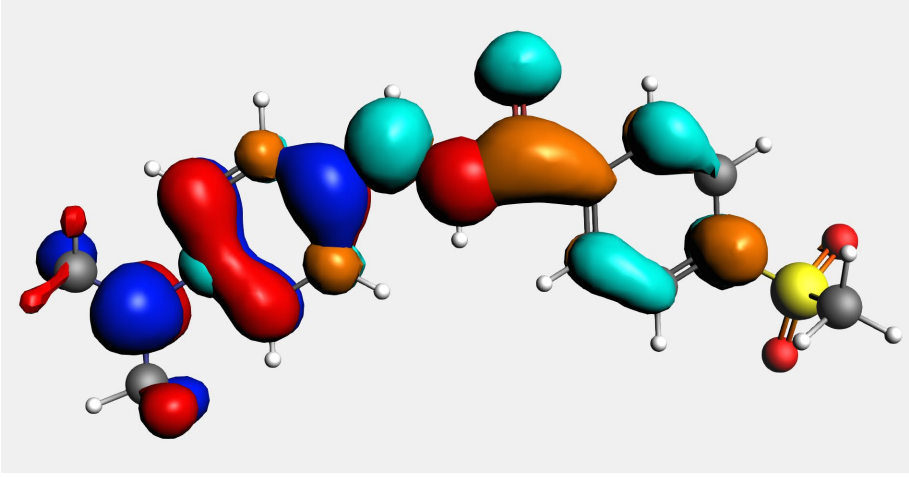

Fig. 10. The molecule orbital HOMO – LUMO excitation diagram of MSPPP.

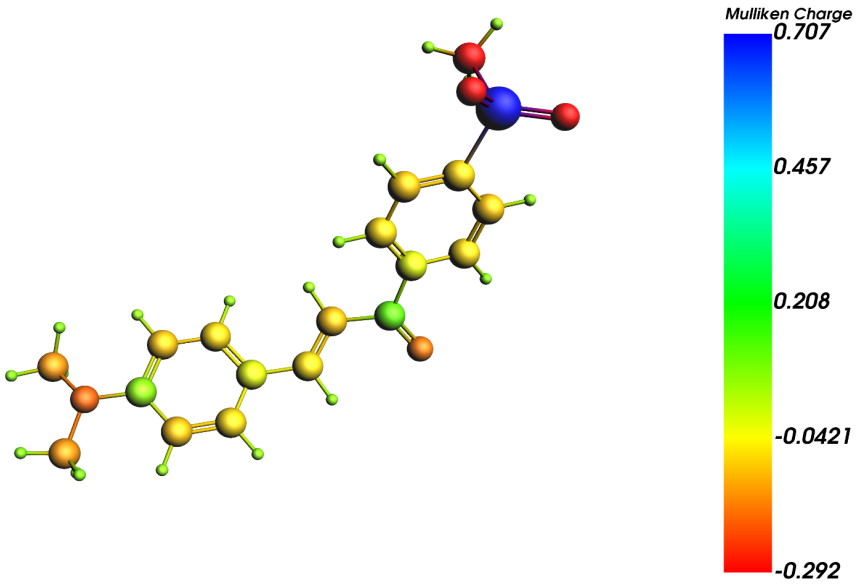

Fig. 11. The Mulliken charges illustrated by the optimized structure of the MSPPP molecule.

4. Conclusions

The spectral and ASE behaviors of MSPPP and coumarin 503 were studied under the influence of concentrations, solvent environments, and laser power excitation levels. The ASE, the Stokes shift, and Quantum yield were investigated. MSPPP showed a strong brightness and green ASE, also showed largely the Stokes shift. The main important properties of MSPPP are: (1) the photochemical stability and the ASE intensity of MSPPP were remarkably high compared with coumarin 503, (2) and according to the variety of solvents, the ASE emission from MSPPP is tunable in the wavelength region between 515 and 548 nm. For MSPPP, the DFT was used to compute the molecular orbitals, total energy, dipole moment, electron charges distribution, and the HOMO–LUMO transitions (1.73 eV energy band-gap).

Author Contributions

All authors effectively participated in this investigation as mentioned below: Conceptualization was carried out by Mohana Attia and Abdelrahman A. Elbadawi; Methodology was done by Mohana Attia; Formal analysis and investigation were carried out by Mohana Attia; Writing original draft preparation was carried out by Mohana Attia; Writing review and editing were carried out by Mohana Attia and Abdelrahman A. Elbadawi. Supervision was done by Abdelrahman A. Elbadawi.

References and Notes

[1] Rao, Y. K.; Fang, S.-H.; Tzeng, Y.-M. *Bioorg. Med. Chem.* **2004**, *12*, 2679. [Crossref]

[2] Jagtap, A. R.; Satam, V. S.; Rajule, R. N.; Kanetkar, V. R. *Dyes and Pigments*. **2011**, *91*, 20. [Crossref]

[3] Sun, Y.-F.; Cui, Y.-P. *Dyes and Pigments*. **2008**, *78*, 65. [Crossref]

[4] Kitaoka, Y.; Sasaki, T.; Nakai, S.; Yokotani, A.; Goto, Y.; Nakayama, M. *Appl. Phys. Lett.* **1990**, *56*, 2074. [Crossref]

[5] Indira, J.; Karat, P.P.; Sarojini, B.K. *Journal of Crystal Growth*. **2002**, *242*, 209. [Crossref]

[6] Sun, S.J.; Schwarz, G.; Kricheldorf, R.H.; Chang, T.C.*J. Polym. Sci., Part A: Polym. Chem.* **2000**, *37*, 1125. [Crossref]

[7] Krohn, K.; Steingröver, K.; Rao, M. S. *Phytochemistry*. **2002**, *61*, 931. [Crossref]

[8] Sato, Y.; Morimoto, M.; Segawa, H.; Shimidzu, T. *J. Phys. Chem*. **1995**, *99*, 135. [Crossref]

[9] Lin, Y.-M.; Zhou, Y.; Flavin, M. T.; Zhou, L.-M.; Nie, W.; Chen, F.-C. *Bioorg. Med. Chem*. **2002**, *10*, 2795. [Crossref]

[10] Kitaoka, Y.; Sasaki, T.; Nakai, S.; Yokotani, A.; Goto, Y.; Nakayama, M. *Appl. Phys. Lett*. **1990**, *56*, 2074. [Crossref]

[11] Lunardi, F.; Guzela, M.; Rodrigues, A. T.; Corrêa, R.; Eger-Mangrich, I.; Steindel, M.; Grisard, E. C.; Assreuy, J.; Calixto, J. B.; Santos, A. R. S. *Antimicrob Agents Chemother*. **2003**, *47*, 1449. [Crossref]

[12] Doroshenko, A. O.; Grigorovich, A. V.; Posokhov, E. A.; Pivovarenko, V. G.; Demchenko, A. P. *Mol. Eng*. **1998**, *8*, 199. [Crossref]

[13] Rurack, K.; Bricks, J. L.; Reck, G.; Radeglia, R.; Resch-Genger, U. *J. Phys. Chem. A*. **2000**, *104*, 3087. [Crossref]

[14] Marcotte, N.; Fery-Forgues, S.; Lavabre, D.; Marguet, S.; Pivovarenko, V. G. *J. Phys. Chem. A*. **1999**, *103*, 3163. [Crossref]

[15] Das, P.K.; Pramanik, R.; Banerjee, D.; Bagchi, S. *Spectrochim. Acta, Part A*. **2000**, *56*, 2763. [Crossref]

[16] Xu, Z.; Bai, G.; Dong, C. *Spectrochim. Acta, Part A*. **2005**, *62*, 987. [Crossref]

[17] Wang, P.; Wu, S. *J. Photochem. Photobiol., A*. **1995**, *86*, 109. [Crossref]

[18] DiCesare, N.; Lakowicz, J. R. *Anal. Biochem.* **2002**, *301*, 111. [Crossref]

[19] Wang, Y. *J. Phys. Chem*. **1985**, *89*, 3799. [Crossref]

[20] Jiang, Y. B.; Wang, X. J.; Lin, L. *J. Phys. Chem*. **1994**, *98*, 12367. [Crossref]

[21] El-Daly, S. A.; Gaber, M.; Al-Shihry, S. S.; El Sayed, Y. S. *J. Photochem. Photobiol., A*. **2008**, *195*, 89. **[Crossref]**

[22] Attia, M. F. *Asian J. Phys. Chem. Sci.* **2019**, *7*, 1. **[Crossref]**

[23] Lippert, E. *Zeitschrift für Naturforschung A*. **2014**, 10, 541. **[Crossref]**

[24] Noboru, M.; Yozo, K.; Masao, K. *Bull. Chem. Soc. Jpn.* **1956**, *29*, 465. **[Crossref]**

[25] Ibnaouf, K. H.; Prasad, S.; AlSalhi, M. S.; Hamdan, A.; Zaman, M. B.; El Mir, L. *J. Lumin.* **2014**, *149*, 369. **[Crossref]**

How to cite this article

Attia, M.; Elbadawi, A. A. *Orbital: Electron. J. Chem.* **2022**, *14*, 82. DOI: **http://dx.doi.org/10.17807/orbital.v14i2.16192**